JOURNAL OF MATERIALS SCIENCE 6 (1971) 25–32

Sintering of MgO: Densification and Grain Growth

TAPAN K. GUPTA
Ceramics and Glasses, Westinghouse Research Laboratories, Pittsburgh, Pennsylvania 15235, USA

The densification rate and grain growth rate of pure MgO powder compacts are measured between 1450 and 1650° C in air. Densification rate in a semilog plot appears to be linear up to about 94% of the theoretical, followed by marked nonlinearity. The time dependence of grain growth is $\frac{1}{2}$ at the beginning and then decreases considerably with further sintering. Application of lattice diffusion model to the densification and grain growth data gives calculated diffusion coefficients in fair agreement with the directly measured diffusion coefficients for magnesium; they are also in fair agreement with the literature value of the diffusion coefficients calculated from various other kinetic processes in MgO.

1. Introduction

Magnesium oxide has been subject to study for densification [1–4] and grain growth [5, 6] by many authors. While pressure sintering [7–10] has attracted major attention in MgO, concurrent studies on densification and grain growth by conventional sintering have not drawn similar attention. The present investigation is aimed at understanding the mechanism of material transport during the late stage of sintering and also to correlate the results with the findings from other kinetic processes.

The analysis of the intermediate stage of sintering presents more difficulty than the initial stage of sintering. This arises primarily from the inability of the intermediate stage model equations to incorporate grain growth kinetics into the equations [11]. However, analysis of the densification data has been carried out in a semiempirical manner by assuming a constant grain size over a short interval of time and the diffusion data thus obtained for copper [11], alumina [11], beryllia [12] and zinc oxide [13] showed fair agreement with the tracer diffusion data; for these materials densification appears to be controlled by lattice diffusion of the rate controlling species. Since rate processes like diffusion, pressure sintering, creep and grain boundary grooving are well characterised in MgO, it was considered to be an ideal material to test further the applicability of the model for the intermediate stage of sintering which was used so successfully for other materials [11–13].

During the analysis of the data of MgO it was found that the model which appears to apply in the intermediate stage is the one for densification by lattice diffusion for grains with cylindrical pores on the edge of a truncated octahedron given by [11]:

$$[f(P)]_1^2 = \left[-1.19 \times 10^3 \frac{D_L \gamma \Omega}{G^3 kT} t \right]_1^2 \quad (1)$$

where $f(P)$ is a function of the volume fraction of porosity P, given by $P^{3/2}[1 + ln\,(8\sqrt{2}P/3\pi)^{-1/2}]$. In equation 1, D_L is the lattice diffusion coefficient, γ the surface energy, Ω the volume of the diffusion species, G the grain size, kT the Boltzmann constant times the absolute temperature and t is the time. Expressions for other grain shapes and alternate flux equations can be found elsewhere [11].

2. Experimental

The magnesium oxide powders were made by precipitation of hydroxide from magnesium chloride and subsequent calcination at 1050° C for 4 h in air. This temperature and time were found to yield powders of strikingly uniform particle size, which was determined by measuring the dimension of a large number of particles from electron micrographs similar to one shown in fig. 1. The approximate particle size is 0.2 μm and they have the shape of regular cubes. The

major cation impurities in ppm as determined by emission spectroscopic analysis are as follows:

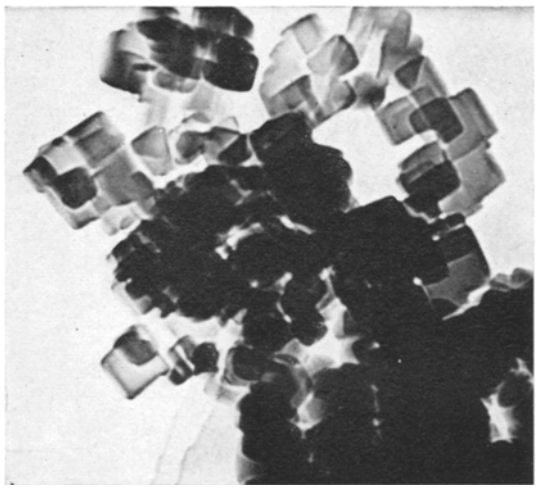

Figure 1 Electron micrographs of MgO powder used in sintering. Average particle size 0.2 microns (× 30 000).

Fe < 10, Cr < 10, Si = 100, Al = 100, Mo < 10, Sn < 50, Cd < 100, Cu = 10, Ti < 10, Mn < 100, Zn < 100.

The calcined powder was screened to − 200 mesh and compacts of about 1 cm diameter and 0.2 cm thick were made by pressing isostatically at a pressure of about 30000 psi without the use of binders. All the samples were then presintered at 900° C for 1 h at a rate of rise of 150° C/h and the samples with densities between 1.66 and 1.67 gm/cm^3 were subsequently sorted out and stored for further experiments. The reproducibility of these samples was within 5%.

The specimens were heated in a tube furnace made of Pt 10 Rh resistance wire and controlled to ± 5° C by a West program controller. The temperature of sintering was between 1450 and 1650° C and the time up to 1000 min. The furnace was raised to the appropriate temperature, the specimens inserted in the furnace in a magnesia boat, heat treated and then taken out of the furnace after the specified sintering time. The specimens were equilibrated with the furnace temperature after insertion for about ½ to 1 min depending on temperature, and appropriate corrections were made for equilibration time so that the heat treatment of the individual samples may be considered isothermal. The samples were then measured for weight and dimensions after grinding the surfaces, when necessary, for parallelism, and the densities were calculated. An average of two to three samples was reported in the data. A further check on densities was made by following the change in densities on a single sample at successive times at temperature and making a correction for the insertion of the samples as usual. The agreement between the two was within 5%. The data reported in the following are from the multiple sample experiments.

Microstructures were developed by polishing and etching with dilute nitric acid and the grain size was determined by counting the number of grain boundaries intersected by measured lengths of random straight lines drawn directly on photomicrographs. The grain size reported is 1.5 times the average intercept length thus obtained by lineal analysis. In addition, fractographic examination of the freshly fractured surface of MgO was conducted over the entire range of experimental data to determine the time and temperature at which the grain growth and thus the intermediate stage of sintering begins. In general it was found that below a relative density of 65% of the theoretical density, regardless of the temperature of sintering, grain growth does not occur to any measurable extent. Densification data below this level also show characteristics differing from those reported in the experiments and are not considered here. The fractographs were also used to determine the grain shape generated during sintering. This in turn fixed the model for specific grain shape to be used in the analysis of the data.

3. Results and Discussion

3.1. Densification and Grain Growth

Isothermal densification in air from 1450 through 1650° C is plotted in fig. 2 as per cent relative density versus log time. Although such plots can claim no theoretical justification, similar plots have been made for other materials [11, 13–15] in the late stage of sintering. A linear relation exists up to about 93 to 95% of the theoretical density followed by marked lowering of densification rate for extended period of time. By comparison with the sintering data of other material [13–15], it is assumed that the linear portions of the curves are associated with the intermediate stage of sintering (continuous pore phase) and equation 1 is applied here; the nonlinear parts are probably associated with the final stage (discontinuous pore phase) of sintering. At 1650° C the final stage is reached in a remarkably

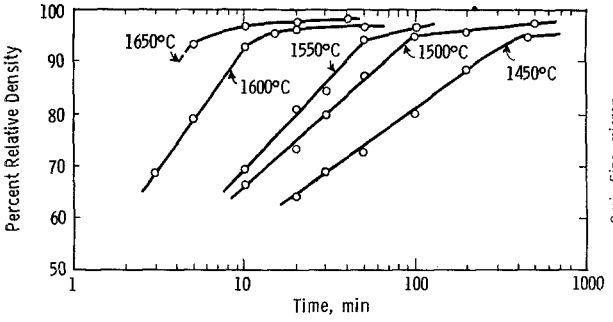

Figure 2 Densification of MgO in air.

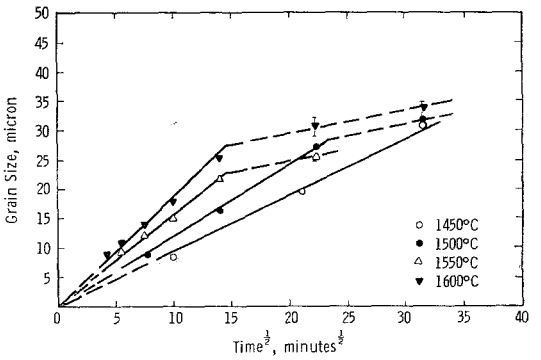

Figure 3 Isothermal grain growth of MgO in air.

short time and the analysis of the intermediate stage data is not extended to this temperature.

The isothermal grain growth rate in MgO is found to fit best by plotting grain size (G) versus time $(t)^{1/2}$ as shown in fig. 3. For most of the porous materials [13–15] the time dependence of grain growth has been found to be equal to $\frac{1}{3}$ as opposed to $\frac{1}{2}$ predicted theoretically [16]. However, the reported data on porous [5] and pressure sintered [6] MgO give the same time dependence for grain growth, $t^{1/2}$. Thus porosity does not seem to have an effect on the normal grain growth kinetics in MgO, although there is an indication of a limiting grain size being reached with porous material as reported by Daniels *et al* [5]; with hot pressed MgO no such limiting grain size was reported [6]. In the present study as seen in fig. 3 there is an indication of a decrease in grain growth rate after a long period of sintering, this time progressively decreasing with increasing sintering temperature. Thus, at 1450°C no decrease in grain growth rate is observed through 1000 min while at 1600° C, the rate decreases after 200 min of sintering. It is believed that the decrease in grain growth rate is caused primarily by the pores which are situated at the grain boundaries and intersections. On examination of the microstructures it appears that although some pores are trapped within the grains as shown in fig. 4a, others are trapped at grain boundaries and intersections as illustrated in fig. 4b. Fig. 4a is an optical micrograph of a randomly polished surface where one can see large grains with trapped pores while fig. 4b is an electron fractograph of the same specimen (heated at 1600° C for 1000 min) where one can see numerous pores located on grain boundaries and intersections of an intergranularly fractured surface. It is therefore expected that the driving force for grain growth will be reduced by a

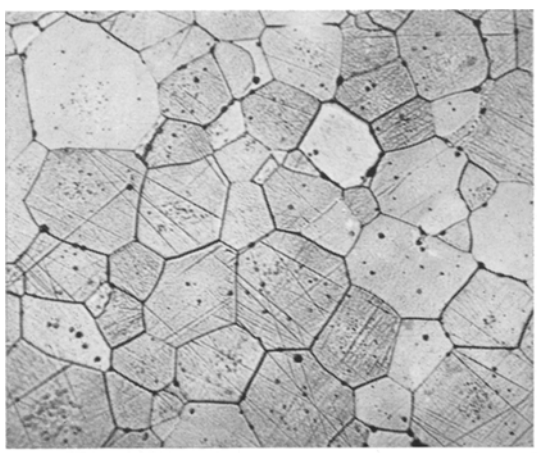

(a)

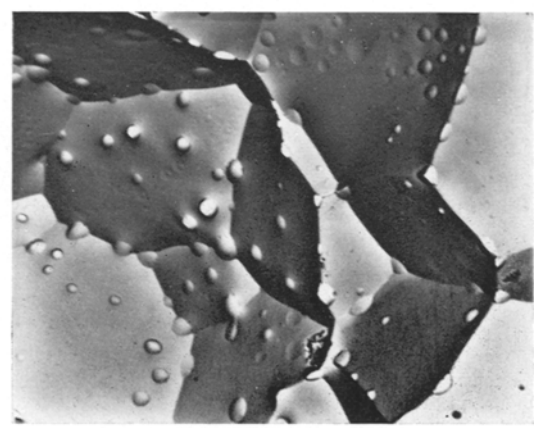

(b)

Figure 4a Optical micrograph of MgO specimen sintered at 1600° C for 1000 min. Note the pores trapped inside the grains (× 500). *4b* Typical fractograph of MgO sintered at 1600° C for 1000 min. Note the pores on grain boundaries and at intersections (× 1800).

quantity [17] proportional to $(1/r - f/r_0)$ where r is that radius of the grain, f the volume fraction of inclusion and r_0 the radius of inclusion. The temperature dependence of grain growth is determined from a plot of the log constant of the grain growth rate (k) of the equation $G^2 = kt$, where G is the grain size at time t, versus reciprocal absolute temperature. The data are illustrated in fig. 5 with an activation energy of

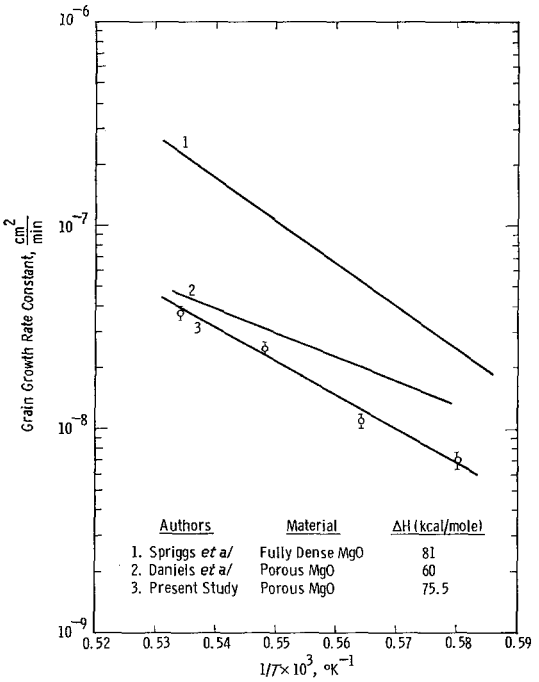

Figure 5 Temperature dependence of normal grain growth of MgO by different authors.

75.5 kcal per mole, which is intermediate between the value reported by Daniels *et al* [5] for porous compacts (60 kcal/mole) and Spriggs *et al* [6] for hot pressed compacts (81 kcal/mole). This high value cannot be identified with any grain boundary migration process; on the contrary it is very close to the activation energy for the lattice diffusion of Mg^{2+} in MgO (79 kcal/mole) [18]. By comparing the growth rate in fig. 5, it is seen that the agreement between the porous MgO compacts as determined by Daniels *et al* [5] and the present study is very good while the growth rate of the fully dense MgO [6] is several times faster than that of the porous MgO. The higher growth rate of the latter is attributed to the absence of porosity [6] which, when present, causes a reduction in the driving force as stated earlier [17]. Thus, porosity appears to limit not only the grain size, but decrease the grain-growth rate as well.

3.2. Diffusion Coefficients

The application of equation 1 to the sintering data requires that grains must conform to the shape of truncated octahedrons (tetrakaidecahedron) [27]. The grain shape was determined by measuring the edge per face of the polyhedron, observed on a large number of fractographs similar to one presented in fig. 4b. The result is illustrated in fig. 6 as a plot of edge per face of the polyhedron per 100 grains versus frequency of occurrence of such edge, measured from the fractographs at different temperatures. It is seen that the maximum edge per face, at all temperatures, falls well within the four-to-six-sided range, an observation so well documented by Smith for a tetrakaidecahedral configuration of grains [19].

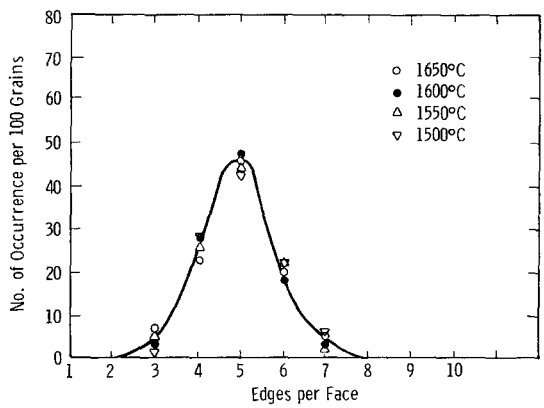

Figure 6 Polyhedral occurrence in MgO microstructure.

Diffusion coefficients are calculated using $\gamma = 10^3$ erg/cm² [20] and $\Omega = 1.86 \times 10^{-23}$ cm³ and is plotted in fig. 7 along with other diffusion data obtained from different sources for comparison. Each point in the figure for the present investigation represents an average of more than ten calculations made from different points on the density and grain size curves between 1450 and 1600° C. The size at short times was obtained by extrapolating the appropriate grain growth curves to short times and assuming that there is no change in the exponent. The resultant points fit the equation:

$$D = 87 \exp\left(-\frac{102 \pm 15}{RT} \text{ kcal}\right) \qquad (2)$$

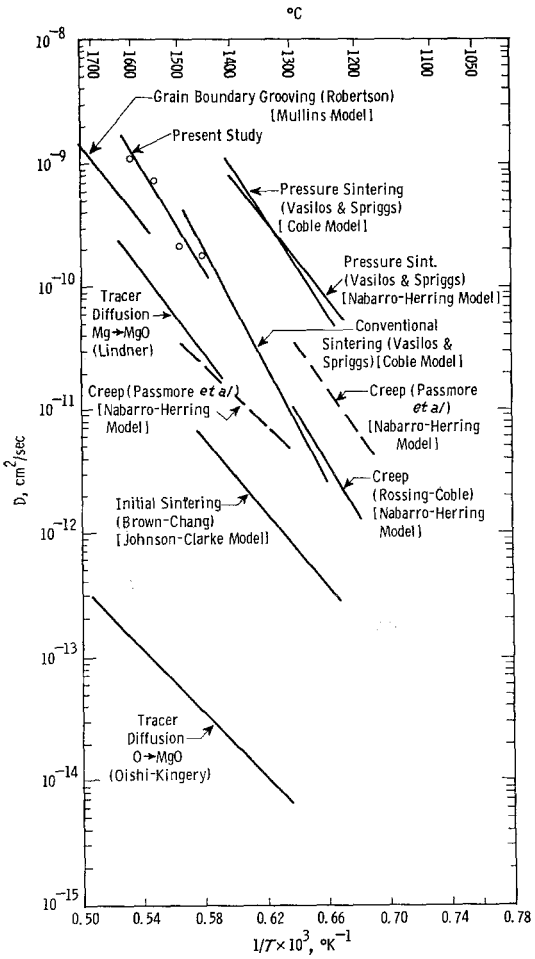

Figure 7 Comparison of tracer diffusion coefficients of MgO with those calculated from conventional sintering, pressure sintering, creep and grain boundary grooving data.

In addition to sintering data of the present investigation, fig. 7 also includes the following: the pressure sintering data of Vasilos *et al* [21], conventional sintering data of Vasilos *et al* [21], grooving kinetics data of Robertson [20], creep data of Passmore *et al* [22] for grain size of 3.6 μm and 18 μm respectively, creep data of Rossing as reported by Coble [23] for grain size of 5 μm, tracer diffusion data of magnesium [18] and oxygen [25] in MgO and initial sintering data of Brown [26] as reported by Chang [32]. These data represent an overall transport behaviour of MgO over a wide range of temperature (1300 to 1750° C) and grain size (1 to 18 μm) as well as single and bicrystals, with various energies of activation. They are all assembled in table I for comparison.

Diffusion coefficients calculated from the pressure sintering data of Vasilos and Spriggs [21] using Coble model [14] (reported data for Coble model is corrected for an error in the numerical constant [8]) and Nabarro-Herring model for lattice diffusion coefficients between 1225 and 1400° C, are identical although varying in activation energies, 95 and 78 kcal/mole respectively, the latter agreeing well with the activation energy for the tracer diffusion of magnesium in MgO (table I). When compared with the conventional sintering data (Coble model) by the same authors, the magnitude of the diffusion coefficients for the latter is found to be lower by an order of magnitude, while the activation energy is increased to 112 kcal/mole. Considering the approximation in calculation this is not a serious discrepancy in activation energy. Furthermore, there is mounting evidence at present that atoms in metal [28], can be made to move 1000 to 10000 times faster than normal by stretching or compressing the material while atomic diffusion is going on. These phenomena in metal are known to occur by diffusion along dislocation pipes, which become better conductors for diffusions when under motion during plastic deformation. In magnesium oxide, up to five additional slip systems can operate at elevated temperature [29], resulting in plastic flow, and rapid diffusion along dislocations as in metal. So the calculated high values for pressure sintering are in line with the atomic behaviour under stress. The conventional sintering data of Vasilos and Spriggs when extrapolated to 1600° C is in remarkable agreement with the diffusion data calculated from the present investigation; the activation energies are also close (112 kcal/mole for Vasilos and Spriggs and 102 kcal/mole for the present experiment). However, Vasilos and Spriggs do not report the grain size data for conventional sintering or the amount of impurities. When these sintering data are compared with the tracer diffusion data [18] of Mg^{2+} in MgO the latter is lower by one order of magnitude from the conventional sintering, and by two orders of magnitude from pressure sintering data, while the oxygen tracer diffusion data [25] are lower by 4 to 5 order of magnitude. Because of the closer agreement between the sintering data and the tracer diffusion data of Mg^{2+} in MgO it is concluded that sintering is controlled by the lattice diffusion of magnesium.

TABLE I Activation energy, temperature range and grain size for sintering, creep, grain boundary grooving and diffusion in MgO

Rate processes	Temperature °C	Grain size (μm)	Activation energy kcal/mole	Reference
Pressure Sintering:				
Coble Model	1125 to 1400	0.8 to 4.5	95	8, 21
Nabarro-Herring Model	1125 to 1400	0.8 to 4.5	78	8, 21
Conventional Intermediate Stage Sintering:				
Coble Model	1200 to 1500	—	112	8, 21
Coble Model	1450 to 1600	3 to 16	102	Present study
Grain Boundary Grooving:				
Mullins Model	1600 to 1700	Bicrystals	79	20, 33
Creep:				
Nabarro-Herring Model	1227	3.6	85.4	22
Nabarro-Herring Model	1427	18	62.4	22
Nabarro-Herring Model	1200 to 1300	4	110	23
Nabarro-Herring Model	1180 to 1260	1 to 3	74	24
Initial Sintering:				
Johnson & Clarke Model	1300 to 1500	0.03	70	26, 32
Tracer Diffusion:				
Mg → MgO	1400 to 1600	Single crystal	79	18
O → MgO	1300 to 1750	Single crystal	62.4	25

The activation energies of sintering, although higher than those reported for tracer diffusion, also show a better agreement with 70 kcal/mole (for Mg^{2+} diffusion on MgO) than with 62.4 kcal/mole (for O^{2-} diffusion in MgO).

The above conclusion is in agreement with other kinetic data in MgO. Robertson [20] has shown that the grain boundary grooving kinetics follow a lattice diffusion mechanism between 1600 and 1700° C with an activation energy of 79 kcal/mole and a diffusion coefficient which is larger by only several factors from the tracer diffusion of magnesium. As shown in fig. 7, this is in good agreement with the sintering data of MgO. Furthermore, the diffusion coefficients calculated from the creep data in the theoretically dense hot pressed MgO for three different grain sizes [22, 23] using Nabarro-Herring model [30] agree with those extrapolated for magnesium, to within an order of magnitude and are higher by orders of magnitude than the diffusion values for oxygen in MgO. Again, the extrapolated values of conventional sintering data to lower temperatures gives agreement within an order of magnitude, with the diffusion data calculated from the creep. The activation energies of creep (table I) with the exception of that for material 18 μm grain size are in satisfactory agreement with the activation energies for sintering and that for tracer diffusion of magnesium. Finally, the initial sintering data between 1300 and 1500° C was calculated by Chang [32] from an analysis of Brown's [26] results. Brown conducted experiment over the whole range of densification between 40 and 90% of the theoretical; Chang considered the initial part of this densification (40 to 65% theoretical) for his analysis. Although the amount of shrinkage selected for analysis is rather high for an initial sintering model, the data presented by Chang may be considered valid for an order of magnitude comparison, in view of the absence of any reported grain growth by Brown. It is seen from the plot in fig. 7, that the data agree well with the extrapolated values of the tracer diffusion and the present sintering data. On the basis of above arguments, the general conclusion is that there exists a fair agreement between D values estimated from various transport processes and those measured for lattice diffusion of magnesium in MgO. The magnitude of diffusivities compared in fig. 7 show a spread of 10^2 while the activation energies reported in table I show a range of $2X$. It is not known whether these scatters are due to (1) the presence of impurities, (2) empiricism of the model, (3) change of mechanism, (4) uncertainties of grain size data, or (5) other. However, the extent to which the impurities may affect the sintering kinetics of MgO can hardly be overemphasised. This was dramatically demonstrated

by Brown [26]. He showed that pure MgO (10 ppm of impurities) exhibited no grain growth up to 1600°C, whereas an addition of 100 ppm of vanadium altered the rate of densification and grain growth at a considerably lower temperature. Similar effects of impurities on other rate processes like diffusion, creep and grain boundary grooving are also expected.

Tracer diffusion data in fig. 7 show that oxygen diffusion in single crystal is several orders of magnitude slower than magnesium diffusion in MgO [25]. On this basis, sintering should be controlled by the lattice diffusion of oxygen, but as we have seen, the sintering rate is quantitatively related to the diffusion of magnesium. It is proposed, therefore, that the oxygen diffusion occurs along grain boundaries, where oxygen diffusivity is assumed to be greater than in the crystal lattice. The evidence for an enhanced boundary diffusion of oxygen in impure MgO at limited temperatures is given by McKenzie [31] from a combination of proton activation oxygen-18 analysis with autoradiography in polycrystalline MgO. A similar conclusion regarding enhanced boundary diffusion of oxygen during sintering has also been reached for Al_2O_3 [14] and ZnO [13].

4. Conclusions

(i) Application of a lattice diffusion model to the intermediate stage of sintering for MgO shows that, under the experimental conditions used, the calculated diffusion coefficients from the sintering data are in fair agreement with the lattice diffusion coefficients directly measured for magnesium.

(ii) The diffusion equation derived from the sintering data can be expressed by the relation

$$D = 87 \exp\left(-\frac{102 \pm 15}{RT} \text{ kcal}\right)$$

between 1450 and 1600° C.

(iii) It is hypothesised that oxygen diffusion during sintering takes place along grain boundaries. This is in agreement with the enhanced boundary diffusion of oxygen observed in impure MgO.

(iv) Diffusion coefficients calculated from the sintering data in MgO as reported here are also in fair agreement with the diffusion coefficients calculated from other atomistic processes, namely, grooving kinetics, creep, pressure sintering and conventional sintering by other authors. The rate controlling mechanism for all these processes is concluded to be the same.

(v) The grain growth rate in MgO follows the kinetics of the theoretical grain growth with grain size varying with $(\text{time})^{1/2}$. This is in agreement with the literature data for porous and hot pressed MgO. The activation energy for grain growth, 75.5 kcal/mole, is found to be in good agreement with the literature data by other authors.

Acknowledgement

Thanks are due to W. D. Straub for helping in the experimental part of the work.

References

1. A. G. ALLISON, *et al*, *J. Amer. Ceram. Soc.* **39** (1956) 151.
2. L. M. ATLAS, *ibid* **40** (1957) 196
3. G. K. LAYDEN and M. G. MCQUARRIE, *ibid* **42** (1959) 89.
4. P. P. BUDNIKOV, *et al*, Translation from "Ognevpory", No. 4 (April 1965) p. 32.
5. A. V. DANIELS, *et al*, *J. Amer. Ceram. Soc.* **45** (1962) 282.
6. R. M. SPRIGGS, *et al*, *ibid* **47** (1964) 417.
7. R. A. J. SAMBELL, *et al*, Report AERE-R-5216, Harwell, UK, September 1966.
8. T. VASILOS and R. M. SPRIGGS, "Pressure Sintering of Ceramics", Progress in Ceramic Science, edited by J. E. Burke, 4 (Pergamon Press, New York, 1966) p. 95.
9. E. CARNALL, JR., *Mat. Res. Bull.* **2** (1967) 1075.
10. W. RHODES, *et al*, "Development and Evaluation of Transparent Magnesium Oxide", Report No. AD 650-621, February 1967.
11. R. L. COBLE and T. K. GUPTA, "Intermediate Stage in Sintering", in "Sintering and Related Phenomena", edited by G. C. Kuczynski, N. A. Hooton, and C. F. Gibbon (Gordon and Breach, New York, 1967) p. 423
12. T. K. GUPTA, "Estimation of Diffusivities from Grain Size During Sintering", presented at the 21st Pacific Coast Regional Meeting, The American Ceramic Society, Pasadena, California, October 24, 1969; for abstract see *Am. Ceram. Soc. Bull.* **47** (1968) 868.
13. T. K. GUPTA and R. L. COLLE, *J. Amer. Ceram. Soc.* **51** (1968) 521.
14. R. L. COBLE, *J. Appl. Phys.* **32** (1961) 793.
15. T. E. CLARE, *J. Amer. Ceram. Soc.* **49** (1966) 159.
16. D. TURNBULL, *Trans. AIME*, **191** (1951) 661.
17. J. E. BURKE and D. TURNBULL, "Recrystallization and Grain Growth", in "Progress in Metal Physics", edited by B. Chalmers, III (Interscience Publishers, New York, 1952) p. 220.
18. R. LINDNER and G. D. PARFITT, *J. Chem. Phys.* **26** (1957) 182.
19. C. S. SMITH, *Met. Rev.* **9** (1964) 1.

20. W. M. ROBERTSON, "Kinetics of Grain Boundary Grooving on MgO", in "Sintering and Related Phenomena", edited by G. C. Kuczynski, N. A. Hooton, and C. F. Gibbon (Gordon and Breach, New York, 1967) p. 215.
21. T. VASILOS and R. M. SPRIGGS, *J. Amer. Ceram. Soc.* **46** (1963) 493.
22. E. M. PASSMORE, *et al*, *ibid* **49** (1966) 594.
23. R. L. COBLE, "Deformation Behavior of Refractory Compounds", in "High Strength Materials", edited by V. F. Zackay (John Wiley & Sons, New York, 1965) p. 706.
24. T. VASILOS, *et al*, *J. Amer. Ceram. Soc.* **47** (1964) 203.
25. Y. OISHI and W. D. KINGERY, *J. Chem. Phys.* **33** (1960) 905.
26. R. A. BROWN, *Amer. Ceram. Soc. Bull.* **44** (1965) 483.
27. T. K. GUPTA, *J. Amer. Ceram. Soc.* **52** (1969) 166.
28. Fundamental Nuclear Energy Research (1965) p. 286.
29. R. J. STOKES, NBS Publication No. 257 (1964) pp. 41-72.
30. C. HERRING, *J. Appl. Phys.* **21** (1950) 437.
31. D. R. MCKENZIE, "Influence of Iron on Oxygen Grain Boundary Diffusion in Periclase Crystals", M.S. Thesis, University of California, Lawrence Radiation Laboratory, Livermore, California, 1965; NASA Accession No. N65-36495, Report No. UCRL-14215, 1965.
32. R. CHANG, "Diffusion Controlled Deformation and Shape Changes in Nonfissionable Ceramics", in "Proceedings of the Conference on Nuclear Applications of Nonfissionable Ceramics, Washington, DC," 9-11 May, 1966, edited by A. Boltax and J. H. Handwerk.
33. W. W. MULLINS, *J. Appl. Phys.* **28** (1957) 333; *Idem, Trans. Met. Soc. AIME*, **218** (1960) 354.

Received 27 July and accepted 18 October 1970